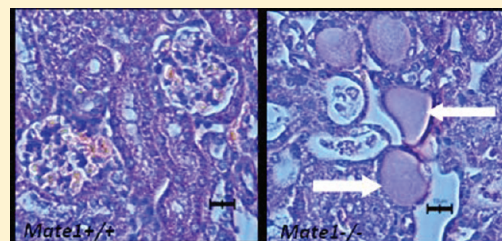


Deficiency of Multidrug and Toxin Extrusion 1 Enhances Renal Accumulation of Paraquat and Deteriorates Kidney Injury in Mice

Qing Li,^{†,‡} Xiujuan Peng,[†] Hyekyung Yang,[†] Hongbing Wang,[†] and Yan Shu^{*,†}[†]Department of Pharmaceutical Sciences, School of Pharmacy, University of Maryland Baltimore, Baltimore, Maryland, United States[‡]Institute of Clinical Pharmacology, Central South University, Hunan 410078, China

ABSTRACT: Multidrug and toxin extrusion 1 (*MATE1*/solute carrier 47A1) mediates cellular transport of a variety of structurally diverse compounds. Paraquat (PQ), which has been characterized *in vitro* as a *MATE1* substrate, is a widely used herbicide and can cause severe toxicity to humans after exposure. However, the contribution of *MATE1* to PQ disposition *in vivo* has not been determined. In the present study, we generated *Mate1*-deficient (*Mate1*^{-/-}) mice and performed toxicokinetic analyses of PQ in *Mate1*^{-/-} and wild-type (*Mate1*^{+/+}) mice. After a single intravenous administration of PQ (50 mg/kg), *Mate1*^{-/-} mice exhibited significantly higher plasma PQ concentrations than *Mate1*^{+/+} mice. The renal PQ concentration was markedly increased in *Mate1*^{-/-} mice compared with *Mate1*^{+/+} mice. The subsequent nephrotoxicity of PQ were examined in these mice. Three days after intraperitoneal administration of PQ (20 mg/kg), the transcript levels of *N*-acetyl- β -D-glucosaminidase (*Lcn2*) and kidney injury molecule-1 (*Kim-1*) in the kidney were remarkably enhanced in the *Mate1*^{-/-} mice. This was accompanied by apparent difference in renal histology between *Mate1*^{-/-} and *Mate1*^{+/+} mice. In conclusion, we demonstrated that *Mate1* is responsible for renal elimination of PQ *in vivo* and the deficiency of *Mate1* function confers deteriorated kidney injury caused by PQ in mice.



KEYWORDS: Paraquat, multidrug and toxin extrusion 1 (*MATE1*/solute carrier 47A1), genetic deficiency, pharmacokinetics, nephrotoxicity

INTRODUCTION

Paraquat (*N,N*-dimethyl-4,4'-bipyridinium dichloride; PQ) is a widely used herbicide due to its rapid effect and quick deactivation once in contact with soil. However, it is of great toxicological importance and associated with a high mortality rate during human exposure.^{1–5} Epidemiological studies also suggest that PQ exposure may increase the risk for Parkinson's disease.^{6,7} PQ accumulates with high concentrations in lung, liver and kidney,^{8,9} which causes the primary symptoms of PQ toxicity, including respiration difficulty, hepatitis, and acute renal failure, respectively.¹⁰ PQ toxicity results from the overproduction of reactive oxygen species.^{11,12} In cells, PQ is first reduced to form free radical monocation (PQ^{•+}) by the reactions mediated by a series of enzymes, including NADPH cytochrome P-450 reductase,¹³ NADPH cytochrome C reductase,¹⁴ the mitochondrial complex I (known as NADH), and ubiquinone oxidoreductase.¹⁵ Subsequently, the monocation is rapidly oxidized while generating abundant superoxide radical (O₂^{•-}).¹⁶ The superoxide radical starts a cascade of downstream reactions leading to the production of reactive oxygen species, mainly hydrogen peroxide (H₂O₂) and hydroxyl radical (HO[•]), which cause DNA damage or genotoxicity, destroy the lipids of cell membranes, and finally induce cell death.¹⁷

PQ is an organic cation with two positive charges and is not metabolized *in vivo*.¹⁸ PQ is predominantly eliminated by urine and, partly, by feces.¹⁹ The capability of organic cation transporters to transport PQ across the basolateral membrane from blood

into the cell and consequently through the apical membrane from intracellular into tubule lumina or bile duct may determine the elimination rate and retention time of PQ *in vivo*. The transporters responsible for transporting organic cations across cellular membrane include organic cation transporters 1–3 (OCT1–3), encoded by solute carrier family 22A 1–3 (*SLC22A1–3*),^{1,20} organic cation/carnitine transporters 1–3 (OCTN1–3), encoded by *SLC22A4*, -5, and -21,²¹ and multidrug and toxin extrusion protein 1–2 (*MATE1–2*), encoded by *SLC47A1* and -2.^{22,23} Human OCT1 is mainly expressed in the liver, while OCT2 in the basolateral membrane of renal proximal tubules.²⁴ In rodents, OCT1 is also abundantly expressed in the kidney.²⁴ OCT3, also called extraneuronal monoamine transporter for its role in the extraneuronal monoamine uptake system (uptake 2), is expressed ubiquitously in most tissues, but with relatively low levels.²⁵ OCTNs are sodium-dependent and high-affinity carnitine transporters. The OCTN1 and OCTN2 expressed in the apical membrane of renal proximal tubules mediate the reabsorption of carnitine and other organic cations to maintain their plasma levels.²⁶ The *MATE* protein family, including *MATE1* and *MATE2* in mammals, has been recently suggested to be responsible for renal or hepatic organic

Received: August 10, 2011

Accepted: September 29, 2011

Revised: September 14, 2011

Published: September 29, 2011

cation elimination or secretion using a H⁺-coupled antiport mechanism.^{27,28}

Limited *in vitro* evidence has suggested that hOCT2, not hOCT1 or hOCT3, hMATE1 and rMATE1 transport PQ in a time- and dose-dependent manner in the overexpression models of HEK-293 cells.²⁹ However, the involvement of these organic cation transporters in the disposition and toxicity of PQ *in vivo* remains undefined. In this study, we generated the mouse model of *Mate1* deficiency (*Mate1*^{-/-}) by the gene trap technique. The toxicokinetics and toxicity of PQ were examined in the *Mate1*^{-/-} and the wild-type mice. Our data indicated that *Mate1* played a critical role in the renal elimination of PQ and disruption of *Mate1* function remarkably potentiated PQ nephrotoxicity in mice.

EXPERIMENTAL SECTION

Materials. Paraquat hydrochloride was purchased from Sigma-Aldrich Co (St. Louis, MO). Paraquat [methyl-¹⁴C] dichloride hydrate (0.1 mCi/mmol) was purchased from American Radiolabeled Chemicals Inc. (St. Louis, MO). [¹⁴C]-Metformin (50 μ Ci, 1.85 MBq) was purchased from Moravak Biochemicals and Radiochemicals Inc. (Brea, CA). All other reagents were commercially available.

Generation of the Mouse Deficient of *Mate1*. The C57BL/6 ES cells with the *Mate1* gene trapped by a retroviral gene trap vector at intron 10 were obtained from the Texas A&M Institute for Genomic Medicine (TIGM, College Station, TX).³⁰ The ES cells were injected into 8-cell embryos isolated from timed pregnant C57BL/6 albino females. Injected 8-cell embryos were cultured to blastocysts and then transferred into the uterus of pseudopregnant females for development into individual pups. Positive chimeric mice were identified by spotted white hairs. The chimeric males were mated with C57BL/6 females to generate F1 offspring from which the germ line transmission of the target allele was confirmed by PCR method. Although the mutant mice were derived from general C57BL/6 background, the mice used in the present study had been backcrossed to C57BL/6J for at least 5 generations to exclude potential subtle genetic background effects.

Animals. All procedures were carried out in accordance with NIH guidelines for animal experimentation, and all experimental protocols were approved by the Institutional Animal Care and Use Committee (IACUC) of the School of Pharmacy, University of Maryland Baltimore. Animals were housed under controlled conditions (21 \pm 2 $^{\circ}$ C, humidity 60 \pm 10% and 12 h/12 h dark/light cycle) and had free access to food and water. All animals used in the present study were male mice with the same genetic background of C57BL/6J, between 12 and 18 weeks of age.

Genomic DNA Extraction and Genotyping. The tail was cut from all offsprings and genomic DNA isolated by QIAamp DNA extraction mini kit (QIAGEN Co., Valencia, CA). The genomic DNA was amplified with two pairs of primers to genotype the mice (one pair for the wild-type allele and the other for the mutant allele: wild-type/mutant forward primer, 5'-GAATGGGTGGCCAAAGTATG-3'; wild-type reverse primer, 5'-CATTGACCTGTCGTGCTGGAT-3'; mutant reverse primer, 5'-CTTGCAAATGGCGTTACTTAAGC-3'). The PCR condition was as follows: an initial 3-min denaturation at 94 $^{\circ}$ C, then 94 $^{\circ}$ C for 30 s, 54 $^{\circ}$ C for 30 s, 72 $^{\circ}$ C for 45 s for 35 cycles, 72 $^{\circ}$ C for 10 min for last extension. The amplified PCR products

were separated in a 2% agarose gel and stained with ethidium bromide.

Reverse Transcription and Real-Time PCR. Total RNA was isolated from the liver and kidney of mice using TRIzol and phenol-chloroform method. The total RNA (2 μ g) was reverse transcribed using a high capability reverse transcript kit (Roche Applied Science, Indianapolis, IN). The reaction mixtures were diluted by 4 times, and 1 μ L was then used as the template for regular PCR or real-time PCR. The regular PCR condition was as follows: an initial 3-min denaturation step at 94 $^{\circ}$ C, then 94 $^{\circ}$ C for 30 s, 54 $^{\circ}$ C for 30 s, 72 $^{\circ}$ C for 10 s for 25 cycles for *Mate1* and glyceraldehyde-3-phosphate dehydrogenase (*Gapdh*) in the liver and kidney. The real-time PCR condition was as follows: an initial 2-min incubation step at 50 $^{\circ}$ C, then 3-min denaturation at 94 $^{\circ}$ C, followed by 40 cycles of 2 steps at 94 $^{\circ}$ C for 30 s and 60 $^{\circ}$ C for 60 s. Real-time PCR was performed on ABI PRISM 7700 (Applied Biosystems, Foster City, CA). The expression of biomarker genes for kidney injury, including *Kim-1* and *Lcn2*, and drug transporters located in the liver and kidney, including *Oct1-3*, *Octn1-3*, *Mrp1-4*, *Oatp1a1*, *Oatp1a4*, *Oatp1b2*, *Mdr1*, *Bcrp*, and *Bsep*, were determined by real-time PCR.

Function Deficiency of *Mate1* in *Mate1*^{-/-} Mice. Metformin has been well characterized as a substrate for *Mate1* *in vitro* and *in vivo*.³¹ In the previous report, metformin pharmacokinetics was significantly altered in the *Mate1* knockout mice created by traditional recombination gene targeting.³² To functionally validate our *Mate1*^{-/-} mouse model, we determined and compared metformin tissue distribution in these mice and wild-type control mice. Five milligrams per kilogram metformin, containing 0.2 μ Ci/mL [¹⁴C]-metformin, was injected *via* tail vein into *Mate1*^{+/+} and *Mate1*^{-/-} mice. At 60 min after injection, different tissues including liver and kidney were removed, weighed, homogenized, and centrifuged. 100 μ L of supernatant was added into scintillation buffer and counted in a multipurpose scintillation counter (Beckman LS6500 Counter, Brea, CA) to determine tissue accumulation of metformin.

PQ Toxicokinetics. In humans, moderate-to-severe poisoning is usually secondary to ingestion of 20–50 mg/kg PQ.³³ In this study, *Mate1*^{+/+} and *Mate1*^{-/-} mice were injected by tail vein with 50 mg/kg PQ as described elsewhere.^{18,33–35} PQ was dissolved in 0.9% saline (the ratio of total paraquat to [¹⁴C]-PQ was 130:1). Blood samples were collected by tail bleeding at 5, 10, 20, 30, 60, and 90 min after injection. The radioactivity in 20 μ L of blood was counted in a multipurpose scintillation counter (Beckman LS6500 counter, Brea, CA). The mice were sacrificed at 90 min, and the tissues were isolated, gently washed, weighed, submerged in phosphate buffered saline, pH 7.4, and further homogenized completely. The homogenized tissues were centrifuged at 15000 rpm for 10 min and the radioactivity in the supernatant was counted.

Determination of Toxicokinetic Parameters. WinNonLin version 5.2.1 (Pharsight Corporation, Mountain View, CA) was used to analyze the plasma concentration–time profiles of PQ after the intravenous administration in mice. Toxicokinetic parameters and the area under the blood concentration–time curve from time 0 to infinity (AUC _{∞}) were calculated by the nonlinear least-squares method. The AUC until 90 min (AUC_{0–90}) was determined by the trapezoidal rule.

PQ Tissue Toxicity. For tissue toxicity experiments, *Mate1*^{+/+} and *Mate1*^{-/-} mice were injected with 20 mg/kg PQ as described elsewhere.^{34,35} PQ was dissolved in 0.9% saline and injected ip. The mice were sacrificed at 72 h after injection. Total

RNA was extracted from one kidney. The expression of *Lcn2* and *Kim-1* genes, as indicators of acute kidney injury,^{36,37} were determined by real-time PCR as described above. For histopathological analysis, the other kidney and the liver were collected and submerged immediately into 10% formalin saline buffer overnight, and further processed to paraffin embedding and hematoxylin and eosin (H&E) staining.

Statistical Analysis. All data were expressed as the mean \pm standard deviation (SD). Data from real-time PCR were analyzed statistically with the one-way analysis of variance (ANOVA) followed by Dunnett's test. Data from blood biochemical analysis and toxicokinetic analysis were analyzed statistically using the unpaired Student's *t* test. A *P* value of <0.05 was considered statistically significant.

RESULTS

Disruption of the *Mate1* Gene by a Gene Trap Vector in Mice. In order to understand the physiology and pharmacology significance of *Mate1*, we generated a *Mate1* mutant mouse strain. The mice were derived from an embryonic stem cell line of mutated *CS7BL/6* ES cell library created by gene trapping in the Texas A&M Institute for Genomic Medicine (TIGM, College Station, TX).³⁰ The ES cell line was integrated with a retrovirus vector containing the 5' selectable marker β -geo, a functional fusion between the β -galactosidase and neomycin resistance genes, in the intron 10 of *Mate1* genomic locus (Figure 1A). Chimeric mice were first generated from ES cells and then mated with wild-type *CS7BL/6J* mice, resulting in germ line transmission. A PCR-based genotyping assay was established to distinguish wild-type, heterozygous, and homozygous mice (Figures 1A and 1B). Heterozygous mice were intercrossed to generate enough wild-type mice and homozygous mutant mice for the following experiments. The *Mate1* transcript level was also determined by real-time PCR in RNA samples from mouse kidney. There was at least 90% reduction in *Mate1* expression in the kidney of mutant mice compared to the wild-type mice (Figure 1C).

Phenotypic Characterization. We monitored all the mice for at least 3 months. We found that there was modest but significant difference in body weight between the wild-type and homozygous mutant mice at 3 months of age (wild-type 25.9 ± 1.14 g vs mutant 30.18 ± 1.57 g, $P = 0.03$, $n = 5$). We did not detect any other overt phenotypes in the homozygous mutant animals. Homozygous mutant mice were observed to be viable and fertile, consistent with previous results of the *Mate1* knockout mice created by gene targeting using homologous recombination.³² Metformin is a well characterized substrate for *Mate1*.³⁸ The accumulation of metformin has been previously demonstrated to be significantly different between wild-type and *Mate1* knockout mice.³² In the present study, the accumulation of metformin in the liver and kidney was determined to functionally validate our mouse model. At 60 min after an intravenous dose of 5 mg/kg metformin, hepatic and renal accumulation was 6.9- and 3.4-fold higher in the homozygous mutant mice than in the wild-type control mice, respectively ($P < 0.05$, Figure 2). The results were comparable to those obtained by others between *Mate1* knockout mice and wild-type mice.³² Based on the results from genotyping, transcript and function measurement, we concluded that the *Mate1* gene was effectively disrupted in our homozygous mutant mice, which are therefore designated as *Mate1*^{-/-} mice.

Drug Transporter Gene Expression in *Mate1*^{-/-} and *Mate1*^{+/+} Mice. To clarify whether mRNA levels of other drug

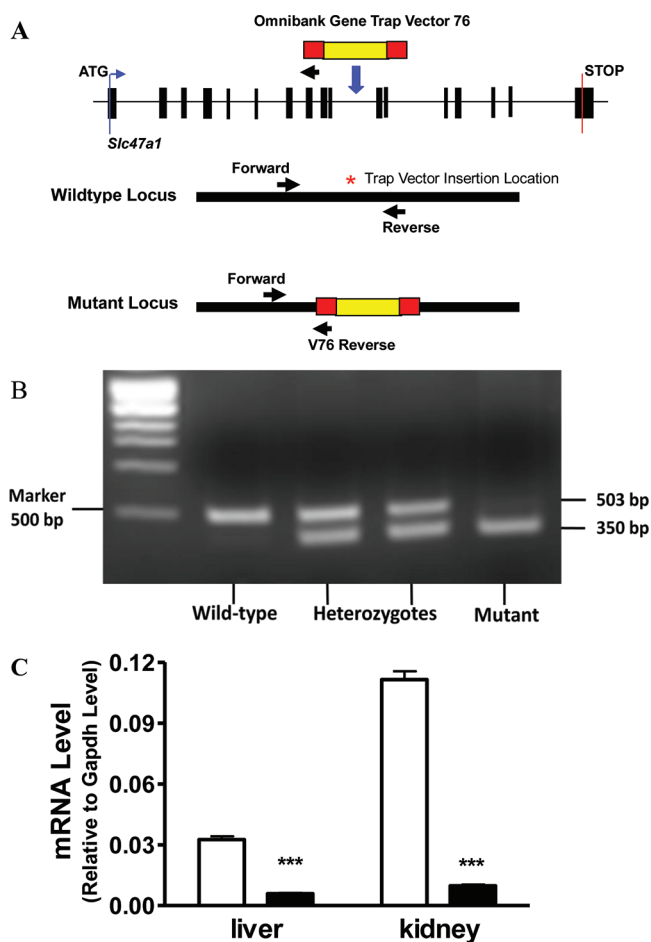


Figure 1. Generation of *Mate1*-deficient mice *via* gene trapping. (A) Schematic of gene trapping and genotyping strategy. Forward and reverse primers are located in intron 10 of *Mate1* genomic locus; V76 reverse primer located in backbone of the trapping vector (Omnibank Gene Trap Vector 76).³⁰ (B) PCR-based genotyping distinguishes wild-type, heterozygous, and homozygous animals. Two polymerase chain reactions (PCR) are needed for genotyping every mouse. The two PCR products were mixed equally and separated at 2% gel with ethidium bromide staining. (C) Transcript levels of *Mate1* in *Mate1*^{+/+} and *Mate1*^{-/-} male mice. The mRNA level shown is relative to that of *Gapdh*. *** $P < 0.001$

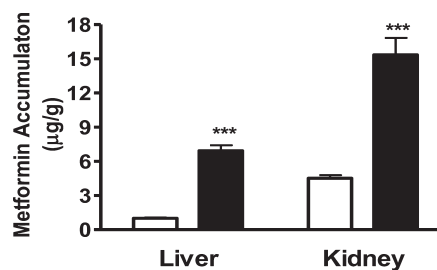


Figure 2. Metformin accumulation in the liver and the kidney of *Mate1*^{+/+} mice and *Mate1*^{-/-} mice. The *Mate1*^{+/+} (white bar) and *Mate1*^{-/-} (black bar) mice were sacrificed at 60 min after the administration of 5 mg/kg metformin containing 0.2 μ ci/ml [¹⁴C]-metformin *via* tail vein injection. Each bar represents the mean \pm SD for 6 male mice. *** $P < 0.001$ significantly different from *Mate1*^{+/+} mice.

transporter genes, in particular organic cation transporter genes, are altered in *Mate1*^{-/-} mice, the mRNA expression of main

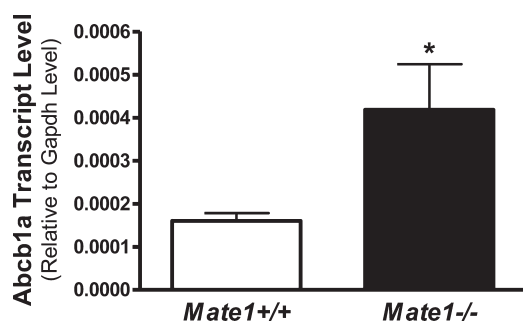


Figure 3. Hepatic *Abcb1a* transcript levels in *Mate1*^{+/+} and *Mate1*^{-/-} mice. The mRNA level shown is relative to the transcript level of *Gapdh*. **P* < 0.05, significantly different from *Mate1*^{+/+} mice.

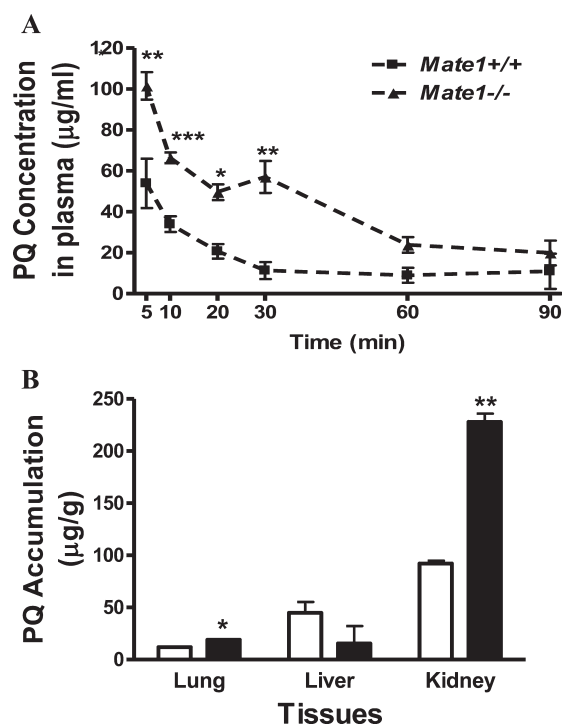


Figure 4. PQ toxicokinetics in the mice of different *Mate1* genotypes. (A) The plasma concentration profile of PQ in *Mate1*^{-/-} (▲) and *Mate1*^{+/+} (■) mice. 50 mg/kg PQ in saline was administered *via* tail vein injection. Blood samples were collected at the time points indicated. PQ levels in the blood samples were determined by counting ¹⁴C-PQ (the ratio of labeled to total PQ is 1:130). Each point represents the mean ± SD for 6 male mice. **P* < 0.05; ***P* < 0.01; ****P* < 0.001, significantly different from *Mate1*^{+/+} mice. (B) PQ accumulation in different tissues from *Mate1*^{+/+} mice (white bar) and *Mate1*^{-/-} mice (black bar) at 90 min after 50 mg/kg PQ administration *via* tail vein injection. Each bar represents the mean ± SD for 6 male mice. **P* < 0.05; ***P* < 0.01, significantly different from *Mate1*^{+/+} mice.

transporters in the kidney and liver was determined by real-time PCR. Except that *Abcb1a* expression was elevated by 150% in the liver of *Mate1*^{-/-} mice (Figure 3), there was no difference in the expression of other transporter genes between *Mate1*^{+/+} and *Mate1*^{-/-} mice (data not shown).

Toxicokinetics of PQ in *Mate1*^{+/+} and *Mate1*^{-/-} Mice. We compared the toxicokinetics of PQ (50 mg/kg), a substrate of *Mate1* identified *in vitro*,²⁹ in *Mate1*^{-/-} and *Mate1*^{+/+} mice. The

Table 1. Toxicokinetic Parameters of PQ in *Mate1*^{+/+} and *Mate1*^{-/-} Mice after 50 mg/kg PQ Injection *via* Tail Vein

parameters	<i>Mate1</i> ^{+/+}	<i>Mate1</i> ^{-/-}	<i>P</i> value
AUC _{0–90} (µg·min/mL)	3380 ± 216	5530 ± 394	0.005
AUC _{0–∞} (µg·min/mL)	7000 ± 2200	9530 ± 2230	0.16
C _{max} (min)	80.5 ± 21.7	127 ± 13.4	0.03
T _{max} (µg/m)	61.8 ± 15.2	84.2 ± 11.4	0.06
T _{1/2} (min)	64.5 ± 9.3	55.2 ± 14.4	0.67

plasma concentrations of PQ were markedly elevated in *Mate1*^{-/-} mice compared with *Mate1*^{+/+} mice (Figure 4A). The AUC_{0–90min} for PQ in *Mate1*^{-/-} was significantly increased 64% when compared with that in *Mate1*^{+/+} mice (5530 ± 394 vs 3380 ± 216 µg·min/mL, *P* = 0.005). C_{max} in *Mate1*^{-/-} and *Mate1*^{+/+} was 127 ± 13.4 and 80.5 ± 21.7 µg·mL/mg, respectively, increasing 57% in the *Mate1*^{-/-} mice (*P* = 0.03). The difference of T_{max} between *Mate1*^{-/-} (84.2 ± 11.4 min) and *Mate1*^{+/+} (61.8 ± 15.2 min) did not reach a statistical significance (*P* = 0.06). The toxicokinetic parameters were summarized in Table 1. The accumulation of PQ in the major tissues including lung, liver and kidney were also measured after the single dose. The renal accumulation of PQ in *Mate1*^{-/-} mice was increased by 147% as compared to the *Mate1*^{+/+} mice (*P* = 0.014). In the lung, PQ accumulation was elevated by 59.5% in *Mate1*^{-/-} mice (*P* = 0.03). However, there was a reversed trend regarding PQ accumulation in the liver. The hepatic accumulation of PQ tended to be lower in *Mate1*^{-/-} mice than in *Mate1*^{+/+} mice (*P* = 0.16) (Figure 4B). Although PQ accumulation tended to be higher in other tissues such as brain, the differences did not reach statistical significance (data not shown).

PQ Toxicity in *Mate1*^{+/+} and *Mate1*^{-/-} Mice. The mice of different *Mate1* genotypes (*Mate1*^{+/+} and *Mate1*^{-/-}) were injected ip with 20 mg/kg PQ. The respiration and behavior activities were observed for 72 h after PQ administration. *Mate1*^{-/-} mice exhibited more difficult respiration, less movement, and decreased body weight in comparison to *Mate1*^{+/+} mice (data not shown). All mice were sacrificed at 72 h. The total RNA was extracted from the kidney and liver. The transcript levels of the *Kim-1* and *Lcn2* genes, as indicators of acute kidney injury,^{36,37} were determined. *Lcn2* expression was apparently elevated by PQ treatment, with much more dramatic increase in the *Mate1*^{-/-} mice when compared with *Mate1*^{+/+} by over 40-fold (*P* < 0.001). Similarly, *Kim-1* expression was 27-fold higher in the *Mate1*^{-/-} mice than that in the *Mate1*^{+/+} mice after PQ treatment (*P* < 0.001) (Figures 5A and 5B). The data indicated that PQ caused more severe acute kidney injury in *Mate1*^{-/-} mice than in *Mate1*^{+/+} mice.

Histopathologic evaluation of kidneys from PQ-treated mice demonstrated much more severe necrosis containing eosinophilic amorphous material and pyknotic debris (depicted by arrows in Figure 6B) in *Mate1*^{-/-} mice than in *Mate1*^{+/+} mice. In addition, *Mate1*^{-/-} kidney showed degeneration including tubular dilatation, tubular cell vacuolation, and tubular cell detachment from basement membrane after the PQ treatment. In the liver, the damage by PQ also showed the same trend as that in the kidney between the two genotypes (Figures 7A and 7B). There was no obvious damage in the liver of *Mate1*^{+/+} mice, while in *Mate1*^{-/-} mice, balloon hepatocytes and apoptotic necrotic cells adjacent to the central vein existed and the basal membrane adjacent to the central vein was inconsecutive and broken.

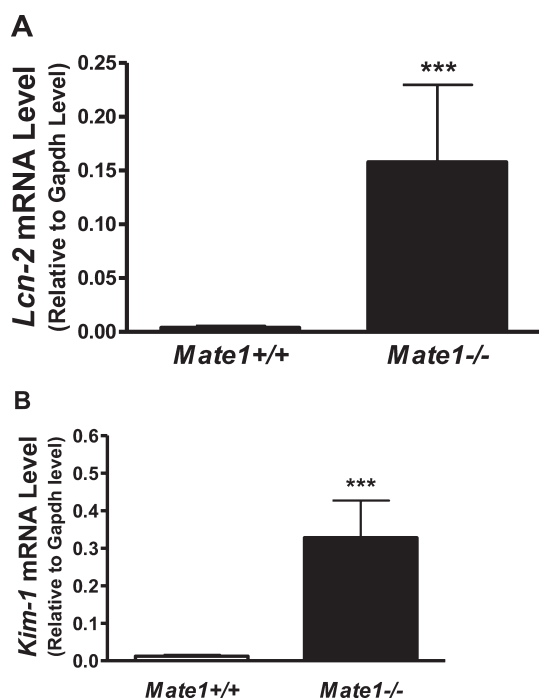


Figure 5. Renal transcript levels of the biomarker genes for acute kidney injury in the mice received PQ treatment. (A) *Lcn2* transcript levels. (B) *Kim-1* transcript levels, in the kidney of *Mate1*^{+/+} (white bar) and *Mate1*^{-/-} (black bar) genotypes, respectively. The mRNA level shown is relative to Gapdh transcript level. ****P* < 0.001, significantly different from *Mate1*^{+/+} mice.

DISCUSSION

In the present study, the mouse model of *Mate1* deficiency was successfully established *via* the gene trap technology. Successful gene trapping was confirmed by using the primers specific to the trap vector and to the *Mate1* genomic locus. *Mate1* transcripts were rarely detected in the kidney and liver of *Mate1*^{-/-} mice, two tissues with high *Mate1* expression in wild-type mice.³⁷ Using metformin as a probe substrate, our *Mate1*^{-/-} mice exhibited loss of *Mate1* transporter function that was comparable to a previous *Mate1* knockout mouse model created by conventional targeting recombination.³² We did not detect any alteration in the expression of other transporters, including those transporting organic cations, except *Abcb1a* encoding P-glycoprotein (P-gp) in the liver. The mouse model of *Mate1* deficiency should be an appropriate tool to characterize the disposition of the xenobiotics interacting with MATE1 *in vivo*.

PQ, a widely used herbicide, is rapidly distributed into tissues and accumulated in the lung, liver and kidney with high concentrations, resulting in serious toxicity in these organs. The kidney is mainly responsible for the elimination of most systemic PQ with minor contribution from the liver.^{18,39} In order to treat patients with PQ poisoning, it is critical to understand the mechanism of PQ elimination in the kidney and preserve renal function. In the *in vitro* overexpression system of HEK-293 cells, PQ has been characterized as a substrate toward OCT2 and MATE1.²⁹ Human OCT2 is primarily expressed at the basolateral membrane and is responsible for the entry of organic cations into the renal proximal tubular cells.¹ In contrast, MATE1 is located in the brush-border membrane and responsible for the second step of renal secretion of organic cations. In the present

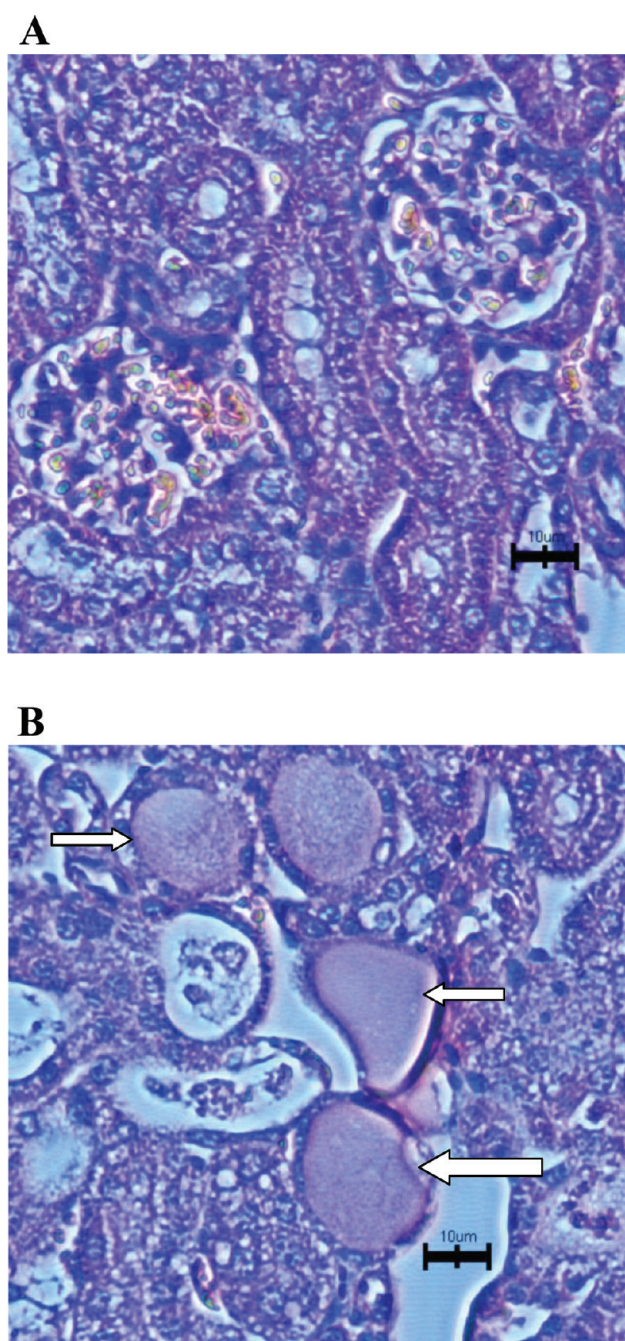


Figure 6. Histopathologic changes in the kidney from the mice received PQ treatment. The *Mate1*^{+/+} (A) and *Mate1*^{-/-} (B) mice were treated with a 20 mg/kg single ip dose for 72 h. *Mate1*^{-/-} kidney shows severe necrosis containing eosinophilic amorphous material and pyknotic debris (white arrows). The black scale bar represents 10 μ m.

study, we sought to determine the role of *Mate1* in determining PQ disposition and toxicity *in vivo* by using our established *Mate1*^{-/-} mouse model. We performed the toxicokinetics of PQ in *Mate1*^{-/-} mice and *Mate1*^{+/+} mice. The concentrations of PQ in the blood were markedly higher in *Mate1*^{-/-} mice compared with *Mate1*^{+/+} mice, along with significant differences in multiple toxicokinetic parameters. The data indicate that *Mate1* plays a critical role in PQ disposition. It should be noted that the *Mate1*^{-/-} mice gained more body weight at 3 months

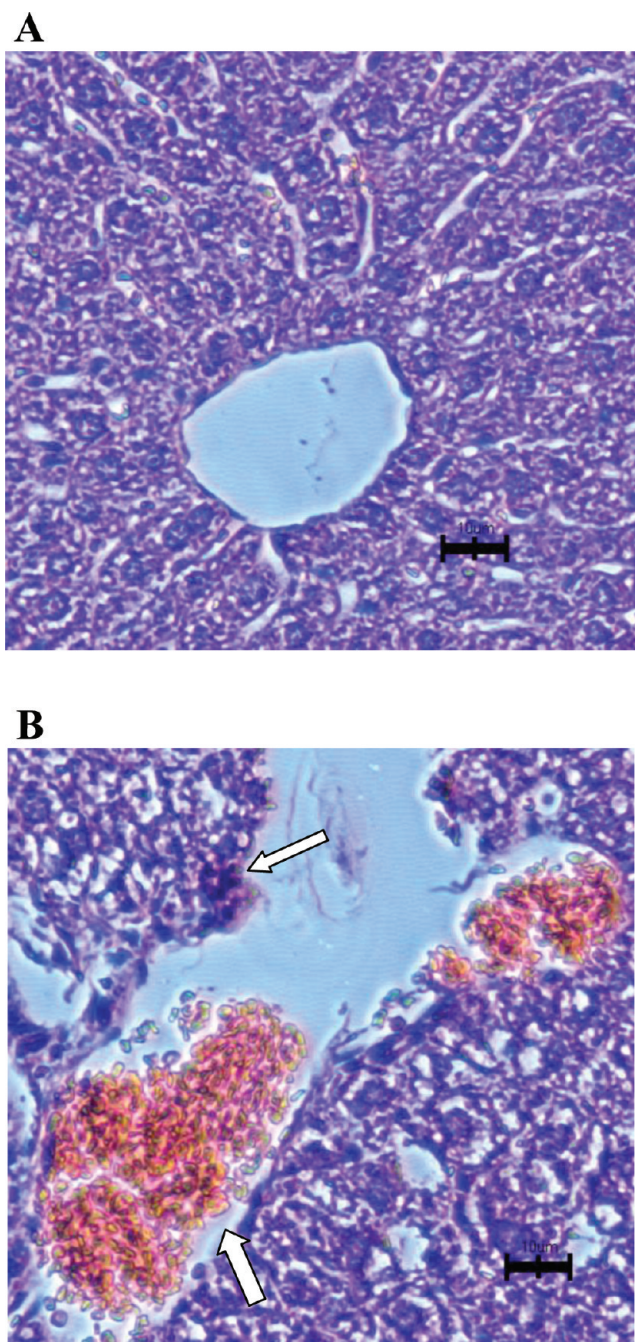


Figure 7. Histopathologic changes in the liver from the mice received PQ treatment. The *Mate1*^{+/+} (A) and *Mate1*^{-/-} (B) mice were treated with a 20 mg/kg single ip dose for 72 h. *Mate1*^{-/-} liver shows balloon hepatocytes and apoptotic necrotic cells adjacent to the central vein and the basal membrane adjacent to the central vein was inconsecutive and broken (white arrows). The black scale bar represents 10 μ m.

of age than wild-type mice. The reason remains to be determined. Currently, there were no reports on effect of body weight on PQ disposition. In this study, PQ was dosed based on the body weight and the reported differences between *Mate1*^{-/-} mice and wild-type mice had been normalized with body weight, suggesting that the toxicokinetic differences between the two genotypes are not secondary to the body weight difference.

PQ accumulation in the kidney and lung, two of the major organs responsible for PQ acute toxicity, was significantly higher for the *Mate1*^{-/-} mice than for the *Mate1*^{+/+} mice after an acute single dose of 50 mg/kg. However, unexpectedly, PQ accumulation in the liver, another major organ responsible for PQ toxicity, tended to, while not significantly, be lower for the former after the acute dose. Since the hepatic accumulation of metformin, a probe substrate of *Mate1*,³⁸ is significantly higher in the mice deficient of *Mate1* function,³² we speculate that the difference in hepatic PQ accumulation between *Mate1*^{-/-} and *Mate1*^{+/+} mice was secondary to *Mate1* deficiency. One possibility is that *Mate1* deficiency caused functional changes for other PQ transporters in the liver. We detected the transcript levels of multiple drug transporter genes in the livers and kidneys from *Mate1*^{-/-} and *Mate1*^{+/+} mice with and without PQ treatment. While PQ treatment seemed to downregulate several transporter genes in the kidney and liver of both *Mate1*^{+/+} and *Mate1*^{-/-} mice, only hepatic *Abcb1a* was found to be differently expressed between these two mice, with *Mate1*^{-/-} mice showing 150% higher expression. P-gp, encoded by *Abcb1a* in mice, is an ATP-driven transmembrane transporter capable of transporting a wide variety of structurally diverse and functionally unrelated compounds out of the cell.⁴⁰ Dinis-Oliveira et al. have reported that the induction of *de novo* synthesis of P-gp by dexamethasone decreases PQ lung accumulation and consequently its toxicity.⁴¹ On the other hand, verapamil, a competitive inhibitor of this transporter, when given one hour before dexamethasone, blocked these protective effects and caused an increase of PQ lung concentration and an aggravation in toxicity.⁴² It is thus likely that the increased *Abcb1a* expression was able to overcome *Mate1* deficiency and responsible for the less or unaltered PQ accumulation in the *Mate1*^{-/-} mice during the studied time. However, this hypothesis needs to be further tested. In particular, it is necessary to directly confirm PQ as a P-gp substrate and determine the mechanism of hepatic *Abcb1a* upregulation secondary to *Mate1* deficiency. It should be noted that *Mate1*^{-/-} mice still exhibited more severe hepatotoxicity than *Mate1*^{+/+} mice after three days of PQ exposure, which may be explained by a much higher systemic PQ exposure over time and/or severe toxicity in other critical organs including kidney and lung.

PQ poisoning can cause acute kidney injury (AKI).³ Kidney injury molecular-1 protein (Kim-1),^{36,43} and lipocalin 2 gene (*Lcn2*), encoding neutrophil gelatinase-associated lipocalin (NGAL),^{37,44} have been demonstrated to be highly upregulated during AKI. They are both primarily potential biomarkers of the early stage of AKI in rodents and humans.^{36,37} We found that the mRNA expression of *Kim-1* and *Lcn2* genes were elevated dramatically in the *Mate1*^{-/-} mice treated by 20 mg/kg PQ for three days, with only marginal increase detected in the *Mate1*^{+/+} mice. Moreover, the histology of kidney and liver showed more severe damage in *Mate1*^{-/-} mice when compared to *Mate1*^{+/+} mice. We also observed apparent toxic symptoms such as respiration difficulty and body weight loss in *Mate1*^{-/-} mice but not in *Mate1*^{+/+} mice. These results, coupled with the toxicokinetic ones, indicated that *Mate1* played a critical role in PQ-induced acute toxicity including AKI by modulation of PQ elimination in the kidney. In humans, MATE1 is highly expressed in the kidney and the liver. MATE2 (MATE2-K) exhibits a kidney-specific expression. MATE1 and MATE2 are detected at similar mRNA levels in human kidney. In mice, *Mate1* is highly expressed in both the kidney and the liver. The tissue distribution of *Mate1* in mice is generally consistent with

that in humans. However, MATE2 is not expressed in mice. Therefore, in the case of MATE, *Mate1*^{-/-} mice may represent a model of deficiency in both MATE1 and MATE2 in human kidney.³²

Previous data suggest a positive dose–response relationship between lifetime cumulative exposure to PQ and risk of PD.^{45–47} Future studies are warranted to use the *Mate1*^{-/-} mice to determine the role of *Mate1* in PQ-induced chronic toxicity such as PD risk. Our data suggest that the toxic response to PQ in patients may vary because of different activity of MATE and that we should avoid the drugs and factors inhibiting MATE function when treating these patients. For example, patients with certain genetic variants of MATE including MATE1 and MATE2 may have different susceptibility to PQ toxicity. Two variants of human MATE1 with no function and four with altered function have been reported.^{48,49} Three of them were polymorphic in a particular ethnic population with allele frequencies greater than 2%. Clinical significance of human MATE polymorphisms in PQ-associated symptoms and diseases merits further investigation.

In summary, we generated a mouse model of *Mate1* functional deficiency by gene trapping. The mouse model can be used to characterize *in vivo* xenobiotic disposition and explore *Mate1* physiology. By using this model, we have demonstrated for the first time that the *Mate1* transporter plays a critical role in the renal elimination of PQ in mice and in conferring PQ toxicity. Future studies are required to define the effect of MATE transporter function on PQ toxicity in humans.

AUTHOR INFORMATION

Corresponding Author

*Department of Pharmaceutical Sciences, School of Pharmacy, University of Maryland at Baltimore, 20 Penn Street, HSF II Room 555, Baltimore, MD 21201, USA. Phone: + 01 410-706-7358. Fax: +01 410-706-7015. E-mail: yshu@rx.umaryland.edu.

ACKNOWLEDGMENT

Dr. Yan Shu receives intramural start-up funds from the School of Pharmacy, University of Maryland Baltimore. Dr. Hongbing Wang receives a research grant from the National Institutes of Health, National Institute of Diabetes and Digestive and Kidney Diseases (Grant No. DK061652).

REFERENCES

- (1) Wright, S. H. Role of organic cation transporters in the renal handling of therapeutic agents and xenobiotics. *Toxicol. Appl. Pharmacol.* **2005**, *204* (3), 309–319.
- (2) Aleksunes, L. M.; Augustine, L. M.; Scheffer, G. L.; Cherrington, N. J.; Manautou, J. E. Renal xenobiotic transporters are differentially expressed in mice following cisplatin treatment. *Toxicology* **2008**, *250* (2–3), 82–88.
- (3) Kimbrough, R. D. Toxic effects of the herbicide paraquat. *Chest* **1974**, *65* (Suppl.), 65S–67S.
- (4) Rogers, P. A.; Spillane, T. A.; Fenlon, M.; Henaghan, T. Suspected paraquat poisoning in pigs and dogs. *Vet. Rec.* **1973**, *93* (2), 44–45.
- (5) Vale, J. A.; Meredith, T. J.; Buckley, B. M. Paraquat poisoning: clinical features and immediate general management. *Hum. Toxicol.* **1987**, *6* (1), 41–47.
- (6) Ascherio, A.; Chen, H.; Weisskopf, M. G.; O'Reilly, E.; McCullough, M. L.; Calle, E. E.; et al. Pesticide exposure and risk for Parkinson's disease. *Ann. Neurol.* **2006**, *60* (2), 197–203.

- (7) Kamel, F.; Engel, L. S.; Gladen, B. C.; Hoppin, J. A.; Alavanja, M. C.; Sandler, D. P. Neurologic symptoms in licensed pesticide applicators in the Agricultural Health Study. *Hum. Exp. Toxicol.* **2007**, *26* (3), 243–250.

- (8) Samai, M.; Sharpe, M. A.; Gard, P. R.; Chatterjee, P. K. Comparison of the effects of the superoxide dismutase mimetics EUK-134 and tempol on paraquat-induced nephrotoxicity. *Free Radical Biol. Med.* **2007**, *43* (4), 528–534.

- (9) Molck, A. M.; Friis, C. Transport of paraquat by isolated renal proximal tubular segments from rabbits. *Pharmacol. Toxicol.* **1998**, *83* (5), 208–213.

- (10) Cristovao, A. C.; Choi, D. H.; Baltazar, G.; Beal, M. F.; Kim, Y. S. The role of NADPH oxidase 1-derived reactive oxygen species in paraquat-mediated dopaminergic cell death. *Antioxid. Redox Signaling* **2009**, *11* (9), 2105–2118.

- (11) Liochev, S. I.; Fridovich, I. The role of O₂⁻ in the production of HO₂[·]: in vitro and in vivo. *Free Radical Biol. Med.* **1994**, *16* (1), 29–33.

- (12) Winterbourn, C. C.; Sutton, H. C. Hydroxyl radical production from hydrogen peroxide and enzymatically generated paraquat radicals: catalytic requirements and oxygen dependence. *Arch. Biochem. Biophys.* **1984**, *235* (1), 116–126.

- (13) Clejan, L.; Cederbaum, A. I. Synergistic interactions between NADPH-cytochrome P-450 reductase, paraquat, and iron in the generation of active oxygen radicals. *Biochem. Pharmacol.* **1989**, *38* (11), 1779–1786.

- (14) Fernandez, A.; Kiefer, J.; Fosdick, L.; McConkey, D. J. Oxygen radical production and thiol depletion are required for Ca(2+)-mediated endogenous endonuclease activation in apoptotic thymocytes. *J. Immunol.* **1995**, *155* (11), 5133–5139.

- (15) Fukushima, T.; Yamada, K.; Isobe, A.; Shiwaku, K.; Yamane, Y. Mechanism of cytotoxicity of paraquat. I. NADH oxidation and paraquat radical formation via complex I. *Exp. Toxicol. Pathol.* **1993**, *45* (5–6), 345–349.

- (16) Ge, W.; Zhang, Y.; Han, X.; Ren, J. Cardiac-specific overexpression of catalase attenuates paraquat-induced myocardial geometric and contractile alteration: role of ER stress. *Free Radical Biol. Med.* **2010**, *49* (12), 2068–2077.

- (17) Niso-Santano, M.; Bravo-San Pedro, J. M.; Gomez-Sanchez, R.; Climent, V.; Soler, G.; Fuentes, J. M.; et al. ASK1 overexpression accelerates paraquat-induced autophagy via endoplasmic reticulum stress. *Toxicol. Sci.* **2011**, *119* (1), 156–168.

- (18) Chan, B. S.; Lazzaro, V. A.; Seale, J. P.; Duggin, G. G. The renal excretory mechanisms and the role of organic cations in modulating the renal handling of paraquat. *Pharmacol. Ther.* **1998**, *79* (3), 193–203.

- (19) Chui, Y. C.; Poon, G.; Law, F. Toxicokinetics and bioavailability of paraquat in rats following different routes of administration. *Toxicol. Ind. Health* **1988**, *4* (2), 203–219.

- (20) Jonker, J. W.; Schinkel, A. H. Pharmacological and physiological functions of the polyspecific organic cation transporters: OCT1, 2, and 3 (SLC22A1–3). *J. Pharmacol. Exp. Ther.* **2004**, *308* (1), 2–9.

- (21) Lash, L. H.; Putt, D. A.; Cai, H. Membrane transport function in primary cultures of human proximal tubular cells. *Toxicology* **2006**, *228* (2–3), 200–218.

- (22) Meyer zu Schwabedissen, H. E.; Verstuyft, C.; Kroemer, H. K.; Becquemont, L.; Kim, R. B. Human multidrug and toxin extrusion 1 (MATE1/SLC47A1) transporter: functional characterization, interaction with OCT2 (SLC22A2), and single nucleotide polymorphisms. *Am. J. Physiol.* **2010**, *298* (4), F997–F1005.

- (23) Ohta, K. Y.; Inoue, K.; Yasujima, T.; Ishimaru, M.; Yuasa, H. Functional characteristics of two human MATE transporters: kinetics of cimetidine transport and profiles of inhibition by various compounds. *J. Pharm. Pharm. Sci.* **2009**, *12* (3), 388–396.

- (24) Alnouti, Y.; Petrick, J. S.; Klaassen, C. D. Tissue distribution and ontogeny of organic cation transporters in mice. *Drug Metab. Dispos.* **2006**, *34* (3), 477–482.

- (25) Duan, H.; Wang, J. Selective transport of monoamine neurotransmitters by human plasma membrane monoamine transporter and organic cation transporter 3. *J. Pharmacol. Exp. Ther.* **2010**, *335* (3), 743–753.

- (26) Iwata, D.; Kato, Y.; Wakayama, T.; Sai, Y.; Kubo, Y.; Iseki, S.; et al. Involvement of carnitine/organic cation transporter OCTN2 (SLC22A5) in distribution of its substrate carnitine to the heart. *Drug Metab. Pharmacokinet.* **2008**, *23* (3), 207–215.
- (27) Masuda, S.; Terada, T.; Yonezawa, A.; Tanihara, Y.; Kishimoto, K.; Katsura, T.; et al. Identification and functional characterization of a new human kidney-specific H⁺/organic cation antiporter, kidney-specific multidrug and toxin extrusion 2. *J. Am. Soc. Nephrol.* **2006**, *17* (8), 2127–2135.
- (28) Tsuda, M.; Terada, T.; Ueba, M.; Sato, T.; Masuda, S.; Katsura, T.; et al. Involvement of human multidrug and toxin extrusion 1 in the drug interaction between cimetidine and metformin in renal epithelial cells. *J. Pharmacol. Exp. Ther.* **2009**, *329* (1), 185–191.
- (29) Chen, Y.; Zhang, S.; Sorani, M.; Giacomini, K. M. Transport of paraquat by human organic cation transporters and multidrug and toxic compound extrusion family. *J. Pharmacol. Exp. Ther.* **2007**, *322* (2), 695–700.
- (30) Zambrowicz, B. P.; Abuin, A.; Ramirez-Solis, R.; Richter, L. J.; Piggott, J.; BeltrandelRio, H.; et al. Wnk1 kinase deficiency lowers blood pressure in mice: a gene-trap screen to identify potential targets for therapeutic intervention. *Proc. Natl. Acad. Sci. U.S.A.* **2003**, *100* (24), 14109–14114.
- (31) König, J.; Zolk, O.; Singer, K.; Hoffmann, C.; Fromm, M. Double-transfected MDCK cells expressing human OCT1/MATE1 or OCT2/MATE1: determinants of uptake and transcellular translocation of organic cations. *Br. J. Pharmacol.* **2011**, *163* (3), 546–555.
- (32) Tsuda, M.; Terada, T.; Mizuno, T.; Katsura, T.; Shimakura, J.; Inui, K. Targeted disruption of the multidrug and toxin extrusion 1 (mate1) gene in mice reduces renal secretion of metformin. *Mol. Pharmacol.* **2009**, *75* (6), 1280–1286.
- (33) Neves, F. F.; Sousa, R. B.; Pazin-Filho, A.; Cupo, P.; Elias Junior, J.; Nogueira-Barbosa, M. H. Severe paraquat poisoning: clinical and radiological findings in a survivor. *J. Bras. Pneumol.* **2010**, *36* (4), 513–516.
- (34) Ecker, J. L.; Hook, J. B.; Gibson, J. E. Nephrotoxicity of paraquat in mice. *Toxicol. Appl. Pharmacol.* **1975**, *34* (1), 178–186.
- (35) Nakagawa, I.; Suzuki, M.; Imura, N.; Naganuma, A. Enhancement of paraquat toxicity by glutathione depletion in mice in vivo and in vitro. *J. Toxicol. Sci.* **1995**, *20* (5), 557–564.
- (36) Wang, E. J.; Snyder, R. D.; Fielden, M. R.; Smith, R. J.; Gu, Y. Z. Validation of putative genomic biomarkers of nephrotoxicity in rats. *Toxicology* **2008**, *246* (2–3), 91–100.
- (37) Wasilewska, A.; Zoch-Zwierz, W.; Taranta-Janusz, K.; Michaluk-Skutnik, J. Neutrophil gelatinase-associated lipocalin (NGAL): a new marker of cyclosporine nephrotoxicity? *Pediatr. Nephrol.* **2010**, *25* (5), 889–897.
- (38) Nies, A. T.; Koepsell, H.; Damme, K.; Schwab, M. Organic cation transporters (OCTs, MATEs), in vitro and in vivo evidence for the importance in drug therapy. *Handb. Exp. Pharmacol.* **2011**, *201*, 105–167.
- (39) Chan, B. S.; Lazzaro, V. A.; Seale, J. P.; Duggin, G. G. Transport of paraquat by a renal epithelial cell line, MDCK. *Renal Failure* **1997**, *19* (6), 745–751.
- (40) Li, Y.; Yuan, H.; Yang, K.; Xu, W.; Tang, W.; Li, X. The structure and functions of P-glycoprotein. *Curr. Med. Chem.* **2010**, *17* (8), 786–800.
- (41) Dinis-Oliveira, R. J.; Remiao, F.; Duarte, J. A.; Ferreira, R.; Sanchez Navarro, A.; Bastos, M. L.; et al. P-glycoprotein induction: an antidotal pathway for paraquat-induced lung toxicity. *Free Radical Biol. Med.* **2006**, *41* (8), 1213–1224.
- (42) Stein, W. D. Kinetics of the multidrug transporter (P-glycoprotein) and its reversal. *Physiol. Rev.* **1997**, *77* (2), 545–590.
- (43) Ko, G. J.; Grigoryev, D. N.; Linfert, D.; Jang, H. R.; Watkins, T.; Cheadle, C.; et al. Transcriptional analysis of kidneys during repair from AKI reveals possible roles for NGAL and KIM-1 as biomarkers of AKI-to-CKD transition. *Am. J. Physiol.* **2010**, *298* (6), F1472–F1483.
- (44) Ferguson, M. A.; Vaidya, V. S.; Bonventre, J. V. Biomarkers of nephrotoxic acute kidney injury. *Toxicology* **2008**, *245* (3), 182–193.
- (45) Liou, H. H.; Tsai, M. C.; Chen, C. J.; Jeng, J. S.; Chang, Y. C.; Chen, S. Y.; et al. Environmental risk factors and Parkinson's disease: a case-control study in Taiwan. *Neurology* **1997**, *48* (6), 1583–1588.
- (46) Nistico, R.; Mehdawy, B.; Piccirilli, S.; Mercuri, N. Paraquat- and rotenone-induced models of Parkinson's disease. *Int. J. Immunopathol. Pharmacol.* **2011**, *24* (2), 313–322.
- (47) Wang, A.; Costello, S.; Cockburn, M.; Zhang, X.; Bronstein, J.; Ritz, B. Parkinson's disease risk from ambient exposure to pesticides. *Eur. J. Epidemiol.* **2011**, *26* (7), 547–555.
- (48) Chen, Y.; Teranishi, K.; Li, S.; Yee, S. W.; Hesselson, S.; Stryke, D.; et al. Genetic variants in multidrug and toxic compound extrusion-1, hMATE1, alter transport function. *Pharmacogenomics J.* **2009**, *9* (2), 127–136.
- (49) Becker, M. L.; Visser, L. E.; van Schaik, R. H.; Hofman, A.; Uitterlinden, A. G.; Stricker, B. H. Genetic variation in the multidrug and toxin extrusion 1 transporter protein influences the glucose-lowering effect of metformin in patients with diabetes: a preliminary study. *Diabetes* **2009**, *58* (3), 745–749.